

Article ID: 1007-4627(2010)04-0399-12

# Delta Excitation in Compressed Neutron-Rich Double Magic Spherical Finite Nucleus $^{132}\text{Sn}^*$

Mohammed H. E. Abu-Sei'leek

(*Department of Physics, Al-Jouf University, Skaka, Saudi Arabia*)

**Abstract:** The ground state properties of  $^{132}\text{Sn}$  at equilibrium and at large compression are investigated, within the framework of the radially constrained spherical Hartree-Fock (CSHF) approximation. The delta resonance effects on the properties of neutron-rich double magic spherical nucleus,  $^{132}\text{Sn}$ , in its ground state and the state under static compression are studied. The sensitivity of the nucleon size and  $\Delta$  model spaces is investigated. At equilibrium, mixing between nucleon and  $\Delta$ 's in the largest model space of nine major nucleon shells plus 10  $\Delta$  orbitals was found. Expanding the nucleon model space has a larger effect on reducing the static compression modulus and softening the nuclear equation of state than increasing the number of  $\Delta$  states. It was found that the most of the increase in the nuclear energy generated under compression is used to create the massive  $\Delta$  particles. For  $^{132}\text{Sn}$  nucleus under compression at 12 times the normal nuclear density, the excited nucleons to  $\Delta$ 's increased sharply up to 13% of the total number of constituents. This result is consistent with the values extracted from relativistic heavy-ion collisions. The single particle energy levels calculated and their behaviors under compression are examined too. A good agreement between results with effective Hamiltonian and the phenomenological shell model for the low lying single-particle spectra is obtained.

**Key words:** nuclear structure; compressed finite nuclei;  $\Delta$ -resonance; Hartree-Fock method; single particle energy

**CLC number:** O571.21      **Document code:** A

## 1 Introduction

A realistic, microscopically derived, nuclear equation of state is of great importance in interpreting the results of high-energy particle-nucleus and nucleus-nucleus collisions. A significant step towards that is to extend the conventional microscopic nuclear model to include delta( $\Delta$ ) resonances in order to incorporate the dynamics associated with the structure of nucleons.

The  $\Delta$  resonance degree of freedom plays an

important role many issues in nuclear physics, such as the nucleon-nucleon scattering, nuclear structure, heavy-ion collisions, and so on.

Compressed nuclei are expected to be occurred during high-energy heavy-ion collisions<sup>[1]</sup>. The issue of compressed nuclei is important in astrophysics. Thus, the problem of compressed nuclei cannot be ignored. Their experimental as well as their theoretical investigation, however, are intricate in particular since the compressed state is hard to realize statically. The theoretical analyses of heavy-

\* **Received date:** 26 Feb. 2010; **Revised date:** 31 Aug. 2010

\* **Foundation item:** Personal Foundation

**Biography:** Mohammed H. E. Abu-Sei'leek (1972-), male (Jordanian Nationality), Zarqa-Jordan, Assistant Professor Dr., working on Nuclear Structure Computational Physics; E-mail: moh2hassen@yahoo.com

ion collisions consequently start from kinetic equations. Nuclei are not infinitely extended and have no stabilizing crystalline background as solids, which can be assumed in band structure calculations of solids. The structure of nuclei with their finite number of particles has to be calculated from extensive many-body problems or simulating an effective nucleon-nucleon(N-N) interaction and transition potentials which are not sufficiently well known.

One of the most fundamental and elusive problems in theoretical nuclear physics has been to understand the structure of finite nuclei in terms of the N-N interaction<sup>[2]</sup>. In conventional non-relativistic microscopic structure calculations, the nucleus is considered as a composite system of elementary particles(protons and neutrons) with no allowed internal degree of freedom. With the advent of high precision experiments at intermediate and high energies using a variety of probes, the contribution of baryon resonances to the structure of nuclei in their ground state and under compression becomes a major experimental and theoretical question<sup>[3, 4]</sup>. For example some relativistic heavy ion collision data show that as much as 10% of the nuclear system can be excited into  $\Delta$  resonances<sup>[5, 7]</sup>. Nucleons are no longer adequately treated as elementary or structureless particles, and the internal dynamics of nucleon has to be taken into consideration. One method that incorporates the dynamics associated with the structure of the nucleons in the nuclear system is to consider the excitations of the nucleon into  $\Delta$  isobars. This excitation can occur as a result of applying an external static load on the nucleus<sup>[8]</sup>. The excitation of  $\Delta$  isobars is very important to understand structure of nuclei at intermediate and high energies. It forms various probes to provide an exciting challenge both theoretically and experimentally, especially in the search for constructive, coherent pion production<sup>[9, 10]</sup>. The  $\Delta$  excitation and its decay to nucleon and pion is current interest in understand light ions, and heavy

ions collision<sup>[11–16]</sup>.

Investigating the delta formation in the nucleus as a function of compression is very important in understanding heavy ion collision problem<sup>[17]</sup>, and astrophysical environments of interest such as supernova explosions or structure of neutron stars<sup>[18]</sup> which are very important in these days in supercolliders when two energetic heavy ions collide. The predictions for highly compressed nuclei at densities accessible to relative heavy-ion collisions are made.

The  $\Delta$  isobar is an important mode of nucleonic excitation. It is due to a resonance in pion-nucleon scattering, photopion and electropion production from nucleon. In nuclear structure, the  $\Delta$  resonance is an agent for corrections in the traditional picture of the nucleus as a system of nucleons only<sup>[19, 20]</sup>. So it considers constituent of nucleus beside nucleons. The  $\Delta$  isobar provides a mechanism for pion scattering, pion production, and pion absorption<sup>[21]</sup>.

Within the framework of constrained spherical Hartree-Fock(CSHF) approximation, in the present work, the  $\Delta$  resonance effects on the properties of the neutron-rich double magic spherical nucleus,  $^{132}\text{Sn}$ , including its ground state and the state under static compression are studied. Heavy nuclei with a large neutron excess develop a neutron skin which is an outer coat of neutron-rich nuclear matter around the core<sup>[22]</sup>. The region of nuclei around doubly-magic  $^{132}\text{Sn}$  is currently a subject of great theoretical and experimental interest<sup>[23]</sup>. The physical interesting of  $\Delta$  resonances is useful for the investigation on the equation of state of dense nuclear matter at high densities where the  $\Delta$  degree of freedom may appear, and this is also a hot topic of the current heavy ion physics research and compact star physics as well<sup>[24]</sup>. Calculations performed using CSHF with a model space of nine major oscillator shells and a realistic effective Hamiltonian<sup>[25]</sup> which contains the N-N, (N- $\Delta$ ), and ( $\Delta$ - $\Delta$ ) interactions. The effective baryon-bary-

on interaction evaluated using the Brueckner  $G$ -matrix<sup>[23, 26–31]</sup>, and its improvement adopted in Refs. [8, 32, 33].

The theory of effective operators plays an important role in the modern approach to nuclear structure. Effective interactions are the basic ingredient of the no-core shell model, one of the methods that provides a solution to the nuclear many-body problem starting from N-N and (N- $\Delta$ ) interactions. Numerical solution to the A-body Schrödinger equation can be obtained only if one truncates the Hilbert space to a finite space, yet sufficiently small dimension. Restriction of the space to a numerically tractable size requires that operators for physical observables be replaced by effective operators that are designed to account for such effects<sup>[34]</sup>.

The results of the role of  $\Delta$ 's in finite nuclei have been investigated<sup>[8, 31–33, 35–44]</sup>. The nucleus has been considered as a collection of nucleons and  $\Delta$ -resonances. The effect of including the  $\Delta$ -degrees of freedom on the Hartree-Fock energy, density distribution,  $\Delta$ -orbital occupations, and single particle energies in the ground state and under low amplitude static compression, and model space consisting of seven major oscillator shells have also been examined. The selected nuclei were:  $^{16}\text{O}$ ,  $^{40}\text{Ca}$ ,  $^{56}\text{Ni}$ ,  $^{90}\text{Zr}$ ,  $^{100}\text{Sn}$ , and  $^{132}\text{Sn}$ .

The main aim of the present work is to study the influence of the model size on finite nuclei properties with the constraint Hartree-Fock approach. In this work, these effects have also been examined into heavy neutron-rich double magic spherical nucleus  $^{132}\text{Sn}$  with a larger amplitude static compression, different model space consisting of nine major oscillator shells with the CSHF approximation, using a realistic effective Hamiltonian with different potential, extensive studies of nuclear density distribution. The Brueckner  $G$  matrices is used which is generated from coupled channels NN, N $\Delta$ , and  $\pi\text{NN}$ <sup>[23, 25–29]</sup>. This is done to give a good description of NN data up to 1 GeV.

The method for calculating the effective interactions of the nuclear shell model<sup>[23, 45]</sup> is being used in this work. It is a good tool to study the highly compressed nuclei at densities accessible to relativistic heavy ion collisions.

This paper is arranged as follows: Sec. 2 specifies the effective Hamiltonian and the model space used in the calculation. The calculation procedure and strategy are outlined in Sec. 3. Results and discussions are presented in Sec. 4. Conclusions will be presented in Sec. 5.

## 2 Effective Hamiltonian $H_{\text{eff}}$ and Model Space

For a nuclear system of A baryons, mass, spin, and isospin of nucleon are:  $m$ ,  $1/2$ , and  $1/2$ , respectively. For  $\Delta$  baryon, the mass, spin, and isospin are:  $M$ ,  $3/2$ , and  $3/2$ , respectively. The intrinsic mass operator Hamiltonian of this system can be written as:

$$H = H_1(\text{one-body}) + H_2(\text{two-body}), \quad (1)$$

where

$$H_1(\text{one-body}) = \left[ \sum_{i=1}^A \frac{p_i^2}{2M} \left( \frac{m-M}{m} \right) + (M-m) \right] \tau_{\text{op}}^{3/2}, \quad (2)$$

here  $p_i$  is the single particle momentum operator,  $\tau_{\text{op}}^{3/2}$  is single particle isospin projection operator and A is the mass number.  $H_1$  arises due to the presence of the  $\Delta$ 's. It consists of a mass correction and a kinetic energy term for the delta particles multiplied by a factor, which is negative since ( $M = 1236$  MeV, and  $m = 939$  MeV). These terms give nonzero contribution in  $\Delta$ -sector only, since projection operator  $\tau_{\text{op}}^{3/2}$  works in the space  $\tau^{3/2}$  only.  $\tau_{\text{op}}^{\tau}$  is single particle isospin projection operator.

$$\tau_{\text{op}}^{\tau} |\tau'\rangle = \delta_{\tau\tau'} |\tau'\rangle, \quad (3)$$

$$\tau_{\text{op}}^{1/2} + \tau_{\text{op}}^{3/2} = 1, \quad (4)$$

$H_2$  is the effective baryon-baryon interaction that consists of the effective N-N interaction that is represented by Reid Soft Core(RSC) potential<sup>[46]</sup> and

the transition potentials among baryons, which are given in details in Ref. [47]. It is given by:

$$H_2(\text{two-body}) = T_{\text{rel}}(m) + V^{\text{BB}'} + V_C, \quad (5)$$

where

$$T_{\text{rel}} = \frac{\sum_{i<j} (\mathbf{p}_i - \mathbf{p}_j)^2}{2mA}. \quad (6)$$

$T_{\text{rel}}$  is the relative kinetic energy operator. Here,  $mA$  is considered total mass of nuclear system,  $V^{\text{BB}'}$  is the strong two-baryon interaction operator and  $V_C$  is the two-particle Coulomb interaction acting between charged baryons.

If the Schrödinger equation is solved in the full infinite Hilbert space of all possible  $N$  and  $\Delta$  many-body configurations, then the exact solution has been gotten, but this is not possible beyond light nuclei with the mass number greater than 16 where special procedure may be adopted<sup>[48–51]</sup>. Therefore, the infinite Hilbert space to finite model space is truncated, and an effective Hamiltonian,  $H_{\text{eff}}$ , to be used in the truncated model space is defined. So, Eq. (5) can be written as:

$$H_{\text{eff}}(\text{two-body}) = T_{\text{rel}}(m) + V_{\text{eff}}^{\text{BB}'} + V_C, \quad (7)$$

Hence  $V^{\text{BB}'}$  in Eq. (5) becomes  $V_{\text{eff}}^{\text{BB}'}$  that is given by:

$$V_{\text{eff}}^{\text{BB}'} = V_{\text{eff}}^{\text{NN}\leftrightarrow\text{NN}} + V_{\text{eff}}^{\text{NN}\leftrightarrow\text{N}\Delta} + V_{\text{eff}}^{\text{NN}\leftrightarrow\Delta\Delta} + V_{\text{eff}}^{\text{N}\Delta\leftrightarrow\text{N}\Delta} + V_{\text{eff}}^{\text{N}\Delta\leftrightarrow\Delta\text{N}} + V_{\text{eff}}^{\text{N}\Delta\leftrightarrow\Delta\Delta} + V_{\text{eff}}^{\Delta\leftrightarrow\Delta\Delta}. \quad (8)$$

The last six terms in Eq. (8) represent all possible transition potentials. The Coulomb term,  $V_C$ , is taken to be the average Coulomb potential energy per proton and  $\Delta^+$  in a uniformly charged sphere:

$$V_C = \frac{6}{5} \frac{Ze^2}{R} \left[ 1 - 5 \left( \frac{3}{16\pi Z} \right)^{2/3} - \frac{1}{Z} \right], \quad (9)$$

where the  $Z^{-(2/3)}$  term is the exchange contribution and the  $Z^{-1}$  term subtracts the interaction of the proton with itself and  $\Delta^+$ .

By applying the variation principle, the Hartree-Fock equation for nucleon and delta orbitals can be derived to use the effective Hamiltonian within the chosen model space. Compression is

achieved by applying a static load. The radial constraint acts like an external force to compress or expand the nucleus. For details see Refs. [35–44].

In calculations, no-core oscillator model space that includes 9 major oscillator shells was used. In the 8-space (9 shells), 37 nucleon orbitals were used:  $0s_{1/2}, 0p_{3/2}, 0p_{1/2}, 0d_{5/2}, 1s_{1/2}, 0d_{3/2}, 0f_{7/2}, 1p_{3/2}, 0f_{5/2}, 1p_{1/2}, 0g_{9/2}, 1g_{7/2}, 1d_{5/2}, 1d_{3/2}, 2s_{1/2}, 0h_{11/2}, 0h_{9/2}, 1f_{7/2}, 1f_{5/2}, 2p_{3/2}, 2p_{1/2}, 0i_{13/2}, 1g_{9/2}, 2d_{5/2}, 0i_{11/2}, 1g_{7/2}, 3s_{1/2}, 2d_{3/2}, 0j_{15/2}, 0j_{13/2}, 1h_{11/2}, 1h_{9/2}, 2f_{7/2}, 2f_{5/2}, 3p_{3/2}, 3p_{1/2}, 0k_{17/2}$  and for delta states, 10 delta orbitals were used:  $0s_{3/2}, 0p_{3/2}, 0p_{1/2}, 0d_{5/2}, 0d_{3/2}, 0d_{1/2}, 1s_{3/2}, 0f_{7/2}, 0f_{5/2}, 0f_{3/2}$ . A total of 47 baryon orbitals were included.

The matrix elements of the effective Hamiltonian had been calculated using the Brueckner  $G$ -matrix method<sup>[23, 25]</sup>. The effective N-N interaction was the sum of the Brueckner  $G$ -matrix and the lowest order fold diagram acting between pairs of nucleons in a no-core model space<sup>[51–53]</sup>. RSC potential for the N-N interaction was adopted.

The constructed effective Hamiltonian in the many-body problem is viewed in the many-body problem to consist of four sectors with matrix elements as follows:

- (1) N-N sector:  $\langle V_{\text{eff}}^{\text{NN}} \rangle + \langle T_{\text{rel}}(m) \rangle + \langle V_C^{\text{pp}} \rangle$ .
- (2) N- $\Delta$  sector:  $\langle V_{\text{eff}}^{\text{N}\Delta} \rangle + \langle V_C^{\text{p}\Delta^+} \rangle$ .
- (3)  $\Delta$ -N sector:  $\langle V_{\text{eff}}^{\Delta\text{N}} \rangle + \langle V_C^{\Delta^+\text{p}} \rangle$ .
- (4)  $\Delta$ - $\Delta$  sector:  $\langle H_1(\text{one-body}) \rangle + \langle T_{\text{rel}}(m) \rangle + \langle V_{\text{eff}}^{\Delta\Delta} \rangle + \langle V_C^{\Delta^+\Delta^+} \rangle$ .

Nucleons to be excited to  $\Delta$ 's from N-N sector were allowed. The picture of the model space which used in this study was completed.

### 3 Calculation Procedure and Strategy

The used strategy was the same of the earlier in Refs. [41–44] and was summarized as a following: First, consider the effective Hamiltonian in the nucleon sector only(i. e. by turning off (N- $\Delta$ )

interaction). This is followed by calculating the ground state properties in the spherical Hartree-Fock approximation (i. e. Hartree-Fock energy,  $E_{\text{HF}}$ , and the root mean square radius( $r_{\text{rms}}$ )) by adjusting the strength of the kinetic and potential factors in  $H_{\text{eff}}$  until agreement between spherical Hartree-Fock results and the experimental binding energy and experimental radius at equilibrium is obtained. The adjusting parameters  $\lambda_1$  and  $\lambda_2$  are introduced to adjust the matrix elements of  $T_{\text{ref}}$  and  $V_{\text{eff}}$ , respectively. Since the two-body matrix elements are evaluated with an oscillator energy spacing  $\hbar\omega = 14$  MeV, these matrix elements are then scaled to the new oscillator basis characterized by new value of  $\hbar\omega'$  as described by Refs. [52–54]. Second, the N- $\Delta$  and  $\Delta$ -N interactions are activated. The adjusting parameters and  $\hbar\omega'$  for  $^{132}\text{Sn}$  nucleus in a given model space at equilibrium with the  $\Delta$  channel turned off are obtained in table 1. Third, the N- $\Delta$  and  $\Delta$ -N interactions are turned off and a radial constraint,  $-\beta r^2$ , is utilized to included static compression. Here,  $r$  is the one-body scalar radius operator. Fourth, the N- $\Delta$  and  $\Delta$ -N interactions are activated and again, the radial constraint,  $-\beta r^2$ , is applied and the difference in  $E_{\text{HF}}$  from the third step and current step as a function of  $r_{\text{rms}}$  is observed.

**Table 1 Adjusting parameters  $\lambda_1$ ,  $\lambda_2$ , and  $\hbar\omega'$  of effective Hamiltonian for  $^{132}\text{Sn}$  for the model space of 9 oscillator shells for which the calculations were performed. The binding energy (point mass radius  $r_{\text{rms}}$ ) that was fitted was  $-1104$  MeV (5.63 fm) for  $^{132}\text{Sn}$**

Nucleus	$\lambda_1$	$\lambda_2$	$\hbar\omega'/\text{MeV}$
$^{132}\text{Sn}$	0.999	1.267	5.361

The computations of this work were done by three major steps; the outline of these steps is presented below.

First, the relative center of mass matrix elements of the transition potentials  $V^{\text{N}\Delta}$  and  $V^{\Delta\text{N}}$  of Refs. [34, 35] evaluated with a computer program

developed for this purpose. The output of the program is the matrix elements in a format suitable for the second step of the calculations. The limits on the relative quantum numbers  $n$ ,  $n'$ ,  $\ell$ ,  $\ell'$ ,  $s$ ,  $s'$ , and the total isospin  $\tau$  are all taken up to 3. The limit on the relative total angular momentum  $g$  is 6. The change in the orbital angular momentum,  $\Delta\ell$ , and spin,  $\Delta s$ , are 0,  $\pm 2$ .

Second, another computer program developed to evaluate the two body matrix elements of the transition potentials in two-particle basis coupled of a good total angular momentum,  $J$ , and total isospin,  $\tau$ . The two-particle basis are constructed from a harmonic oscillator single particle states (nucleon orbitals and  $\Delta$ -orbitals), which are characterized by the quantum numbers  $n$ ,  $\ell$ ,  $s$ ,  $j$ ,  $\tau$ . The relative center of mass transition matrix elements calculated in the first step are read in, and each matrix element undergoes a set of tests to show whether it is required by the constructed two-particle states. If it passes all the tests, then it is stored with an identifying code number. These matrix elements will be multiplied by the appropriate transformation coefficients. The calculations for these steps based on Eq. (13) in Ref. [36]. The matrix elements are evaluated in a no-core model space consisting of nine major oscillator shells (i. e. 37 nucleon orbitals), and ten  $\Delta$ -orbitals. The output of this program served as an input for the third step; the constraint spherical Hartree-Fock calculations.

Third, a spherical Hartree-Fock computer program has been developed to perform the calculations for this phase according to Eqs. (33, 34) in Ref. [36]. An outline of the main processes in one iteration of CSHF calculations is as following; the information is read and stored; the number of particles, number of single particle states, number of Hartree-Fock occupied states and their  $2j$  values, the  $2j$ ,  $\ell$ , and  $n$  values of the harmonic oscillator orbitals,  $\hbar\omega$ ,  $\hbar\omega'$ , and the number of iteration.

The first quantities to be calculated and stored

are the Hartree-Fock Hamiltonian matrix elements  $\langle B|H|B'\rangle$ , according to Eq. (33) in Ref. [36]. To do that, baryon densities of value unity are read and stored. The appropriate two-body matrix elements of the effective Hamiltonian, which were pre-calculated and stored in stage two, are retrieved. The computer code is designed such that if it encounters a two-body matrix elements in the N-N sector, it retrieves a previous calculated  $G$ -matrix elements, the kinetic energy,  $T_{\text{rel}}$ , matrix elements, and the Coulomb energy matrix elements are scaled as mentioned before. The set of Hartree-Fock Hamiltonian matrix elements is used to calculate a second set of Hartree-Fock matrix element  $\langle B|H|B'\rangle'$ , which includes the constraint term and is defined by:

$$\langle B|H|B'\rangle' = \langle B|H|B'\rangle - \beta\langle B|r^2|B'\rangle. \quad (10)$$

This second set of Hartree-Fock Hamiltonian matrix elements is used to calculate the corresponding eigenvalues and eigenvectors. The eigenvectors in turn are used to calculate new baryon densities and the number of  $\Delta$ -particles in the occupied orbitals. The new baryon densities are used to calculate the  $r_{\text{rms}}$ .

Finally, the Hartree-Fock energy,  $E_{\text{HF}}$ , is calculated according to Eq. (34) in Ref. [36]. This is the end of the first iteration. The second iteration starts with the baryon densities calculated in the first iteration and proceeds as the first iteration to calculate the described quantities. The self consistent process continues until a convergent solution is achieved.

## 4 Results and Discussion

In Refs. [33, 38, 39, 44], some selected results for  $^{132}\text{Sn}$  demonstrating the behavior of self-consistent single-particle spectra as a function of compression were presented in the case of small model space. In the present work, more detailed results for  $^{132}\text{Sn}$  are presented in order to examine its properties under static compression in large

model space. The N- $\Delta$  and  $\Delta$ - $\Delta$  interaction were employed as they were activated in a model space consisting of nine major oscillator shells (excluding  $\ell > 5$ ) for nucleons and ten orbitals for  $\Delta$ 's making a total of 47 baryons orbitals.

The differences among the results obtained here and those of previous studies [33, 38, 39, 44] is the size of the nucleon model space, the number of the  $\Delta$  orbitals included and more compression.

The performed calculations were done for  $^{132}\text{Sn}$ . The Hartree-Fock energies,  $E_{\text{HF}}$ , versus  $r_{\text{rms}}$  using RSC potential are displayed in Fig. 1. Fig. 1 clearly shows that there is virtually no difference in the results with and without  $\Delta$ 's at equilibrium. It is seen that without the  $\Delta$ -degree of freedom in the system,  $E_{\text{HF}}$  increases steeply towards zero binding energy under compression. As the volume of nucleus decreased (based on the rms radius) by about 50%, the binding energy will be about 462.67 MeV, when  $\Delta$ -excitations are included at the results obtained when nucleons are considered only. That means, it shows about 727.33 MeV, and 264.66 MeV of excitation energy to achieve a 50% volume reduction in the nucleon-only results, and nucleons and  $\Delta$ 's results, respectively.

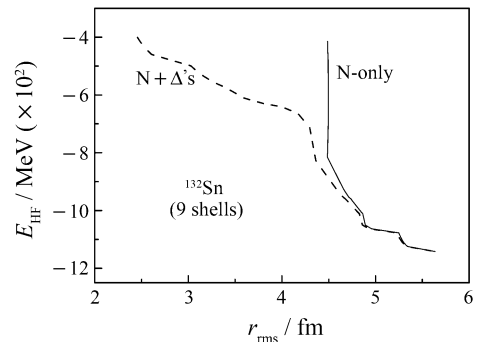


Fig. 1 CSHF energy as a function of the point mass  $r_{\text{rms}}$  using RSC potential for  $^{132}\text{Sn}$  evaluated in 9 major oscillator shells with 10  $\Delta$ -orbitals. The dashed curve corresponds to CSHF full calculations including the  $\Delta$ 's while the solid curve corresponding to CSHF with nucleons only.

It is appeared from the above results, it costs 264.66 MeV of excitation energy to reduce the vol-

ume by 50% and the same amount of energy to reduce it by 24% more. This suggests that the less dense outer part of the nucleus initially responds to the external load more readily than the inner part.

It can be seen from Fig. 1, 741.19 MeV of excitation energy to achieve a 92% volume reduction when the  $\Delta$ -degree of freedom included in the system. The most of this energy go to create massive  $\Delta$  particles.

The differences among the results of the Hartree-Fock binding energy obtained here and those in previous studies<sup>[33, 38, 39]</sup> is the size of the nucleon model space, the number of the  $\Delta$  orbitals included, different potentials, and more compression here. Also it is worth mentioning that at equilibrium (no constraint) in  $^{132}\text{Sn}$ , it was found mixing between nucleon states and the  $\Delta$  states. As the same as in Refs. [33, 38, 39], all curves of  $E_{\text{HF}}$  agree near equilibrium, ( $r_{\text{rms}} = 5.63$  fm). This is implied that the results for the system at equilibrium don't depend on model space. In comparison with the results in Refs. [33, 38, 39], the current results are consistent with the results obtained for  $^{132}\text{Sn}$  for  $E_{\text{HF}}$  with different model space, but the curve of N-only is very steeply. This is due to considering the smallest model space, so the static compression modulus is increased significantly by reduced the nucleon model space. The current results show more compression than the previous studies. The results show that there is a significant reduction in the static compression modulus, for RSC static compressions is reduced by including the  $\Delta$  excitations at large model space. The consequence of this reduction is a softening of the nuclear equation of state at larger compression.

It is shown from Fig. 1, as the static load force increases, the compression of nucleus that has nucleons only is less than the other nucleus has nucleons and  $\Delta$ 's. This result suggests that there is considerable reduction in the compressibility with the  $\Delta$ -degrees of freedom are included.

One potential consequence of this result is that

it could represent a collective mechanism for "Sub-threshold" pion production. That is, in "sub-threshold" pion production experiments between colliding nuclei, if the collision produce isothermal compression, then the  $\Delta$ 's is populated and relaxation could occur by decay of the  $\Delta$ ' to a nucleon and a pion.

To get an impression of the role of the  $\Delta$ 's as a function of compression, the number of  $\Delta$ 's against  $r_{\text{rms}}$  radius was plotted in Fig. 2. The total number of  $\Delta$ 's, the number of  $\Delta^+$ 's and  $\Delta^0$ 's are separately shown.

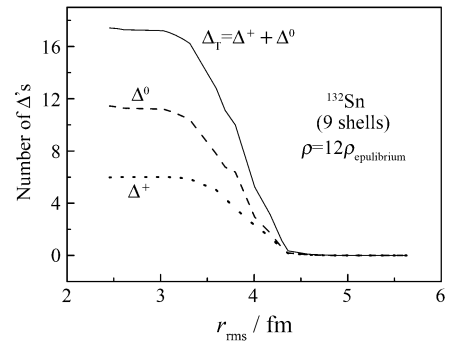


Fig. 2 Number of  $\Delta$ 's as a function of  $r_{\text{rms}}$  for  $^{132}\text{Sn}$  in nine major shells model space. The upper curve is for the total number of  $\Delta$ 's. The dotted curve is for the number of  $\Delta^+$ , and the dashed curve is for  $\Delta^0$ .

In Fig. 2, the number of deltas increases rapidly as volume decreases. When the nucleus volume is reduced to about 92% of its volume at equilibrium, the number of deltas increases to about 13% of all constituents of  $^{132}\text{Sn}$ . It is interesting to note in Fig. 2 that the numbers of  $\Delta^0$ 's and  $\Delta^+$ 's are different as increasing compression. The creation of  $\Delta^0$ 's becomes more favorable as the compression continues. This is due to the number of neutrons is greater than the number of protons. When 17  $\Delta$ 's are presented, the excitation energy values are around of  $17(M-m) \approx 5049$  MeV. Thus, on the scale of the unperturbed single-particle energies, a substantial fraction of the compressive energy is delivered, through the N- $\Delta$ ,  $\Delta$ -N, and  $\Delta$ - $\Delta$  interactions, to create more massive baryons in the lowest energy configuration of the nucleus. By an-

other way, the number of  $\Delta$ 's can be increased to about 17 at  $r_{\text{rms}} = 2.46$  fm which corresponding to about 12 times of normal density.

It can be shown from Fig. 2, the number of  $\Delta$ 's is increased until  $r_{\text{rms}} = 3.1$  fm. After this radius, the number of  $\Delta$ 's becomes constant. The number of  $\Delta^0$  is greater than that of  $\Delta^+$  by about 50% at this radius and this difference stills constant during compression. This is because converted rate from nucleon states to  $\Delta$  states becomes constant in this case. This is major difference from the previous studies<sup>[33, 38, 39, 44]</sup> due to large compression.

In other words, Fig. 2 shows that the number of created  $\Delta$ 's increases sharply, when  $^{132}\text{Sn}$  nucleus is compressed to a volume of about 0.92 of its equilibrium size. However, at this nuclear density, which is about of 12 times the normal density, the percentage of nucleons converted to  $\Delta$  is only about 13% in  $^{132}\text{Sn}$ .

The results show that the total number of  $\Delta$ 's of about  $4 \times 10^{-4}$  is presented in  $^{132}\text{Sn}$  in the ground state at equilibrium (zero constraint). This is perhaps the most notable feature in the  $^{132}\text{Sn}$  results, and in contrast with all previous results<sup>[33, 38, 39, 44]</sup>. This strongly motivates future efforts to proceed to heavier nuclei such as  $^{208}\text{Pb}$ .

To compare results in Fig. 10 of Ref. [33], Fig. 3 of Ref. [38] and Fig. 4 of Ref. [39] with present results in Fig. 2, the number of  $\Delta$ 's increases as the model space decreases. From Fig. 10 in Ref. [33], the creation of  $\Delta$ 's becomes more favorable as the compression continues as model space decreases. The current results in this work show a major difference than those in other findings<sup>[33, 38, 39]</sup>; the number of  $\Delta$ 's at  $r_{\text{rms}} = 4.4$  fm increase very sharply at this radius. This behavior may be artifacts of the small number of  $\Delta$ -orbitals employed, and may be due to the small gap between the  $n = 0$  and  $n = 1$  single particle energies. As moving to larger compression, including the  $\Delta$  states reduces the static compression modu-

lus, but their role in reducing the static modulus is less dramatic than enlarging the size of the nucleon model space. The role of  $\Delta$  states in reducing the static compression modulus is the largest in the smallest space.

In terms of relativistic heavy-ion collisions, the nucleus that can more easily penetrate when the  $\Delta$  degree of freedom becomes explicit is implied by Fig. 1. Because of the limitations of the model space, the calculations for higher densities are more speculative. Nevertheless it can give us some idea about how the  $\Delta$  population can be increased as the nucleus is compressed to higher densities accessible to relativistic heavy-ion collisions. The results shown in Figs. 1 and 2 are consistent with the results extracted from relativistic heavy-ions collisions<sup>[55–57]</sup>.

The results in Fig. 2 that show the gap between number of  $\Delta^0$  and  $\Delta^+$  increases as model space and compression increases. It can be seen, the increase rate of the number of  $\Delta^0$ 's is approximately constant when model space is increased. The creation of  $\Delta^0$ 's becomes more favorable as the compression continues than that of  $\Delta^+$ 's as model space decreases. As moving to larger compression, including the  $\Delta$  states reduces the static compression modulus, but their role in reducing the static modulus is less dramatic than enlarging the size of the nucleon model space. The role of  $\Delta$  states in reducing the static compression modulus is the largest in the smallest model space.

Fig. 3 shows the radial density distribution for  $^{132}\text{Sn}$  at equilibrium state (no constraint) at  $r_{\text{rms}} = 5.63$  fm. It can be seen from this figure, there exists aradial density distribution peak of delta at equilibrium state, at  $r = 3.80$  fm, without compression. This result is appeared during increasing model space.

Fig. 4 displays the radial density distribution of neutrons  $\rho_n$ , protons  $\rho_p$ , deltas  $\rho_\Delta$ , and their sum  $\rho_T$  as a function of the radial distance from the center of the nucleus for  $^{132}\text{Sn}$  at large compression



and point mass radius  $r_{\text{rms}} = 4.58$  fm in a model space of nine major oscillator shells with  $\Delta$  excitation restricted to the ten orbitals:  $0s_{3/2}$ ,  $0p_{3/2}$ ,  $0p_{1/2}$ ,  $0d_{5/2}$ ,  $0d_{3/2}$ ,  $0d_{1/2}$ ,  $1s_{3/2}$ ,  $0f_{7/2}$ ,  $0f_{5/2}$ ,  $0f_{3/2}$ .

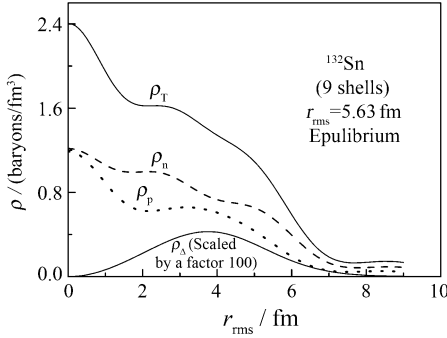


Fig. 3 Total  $\rho_T$ , proton  $\rho_p$  (dotted line), neutron  $\rho_n$  (dashed line), and delta  $\rho_\Delta$  radial density distribution for  $^{132}\text{Sn}$  at equilibrium (point mass radius  $r_{\text{rms}} = 5.63$  fm) in a model space of nine major oscillator shells.

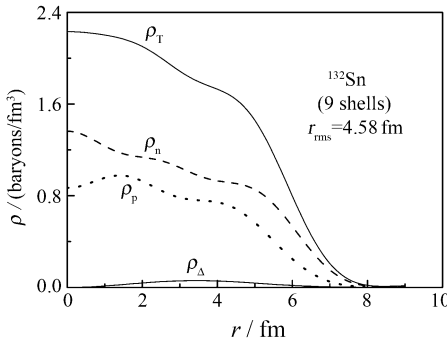


Fig. 4 Total  $\rho_T$ , proton  $\rho_p$  (dotted line), neutron  $\rho_n$  (dashed line), and delta  $\rho_\Delta$  radial density distribution for  $^{132}\text{Sn}$  at point mass radius  $r_{\text{rms}} = 4.58$  fm in a model space of nine major oscillator shells.

From this figure, the neutron radial density is higher than the proton density at all values of  $r$ . This is due to Coulomb repulsion between the protons. At equilibrium, the  $\Delta$ -radial density distribution, under high compression (point mass  $r_{\text{rms}} = 4.58$  fm), reaches a peak value of about 0.01 of the proton radial density at  $r = 3.70$  fm.  $\Delta$ -mixing with the nucleons in the  $0p_{1/2}$ ,  $0p_{3/2}$ ,  $0d_{3/2}$ ,  $0d_{1/2}$ ,  $0f_{7/2}$  and  $0f_{5/2}$  orbitals occurs which explains the shape of the  $\Delta$ -radial distribution presented in Fig. 4.

Fig. 5 displays the radial density distributions of  $^{132}\text{Sn}$  evaluated at an about 0.31 reduced volume ( $r_{\text{rms}} = 3.80$  fm). In this case, the  $\Delta$ -radial density distribution reaches a peak value of about 0.41 of the proton radial density at  $r = 3.3$  fm.

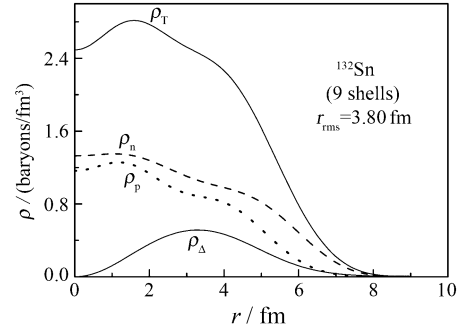


Fig. 5 Total  $\rho_T$ , proton  $\rho_p$  (dotted line), neutron  $\rho_n$  (dashed line), and delta  $\rho_\Delta$  (dotted line) radial density distribution for  $^{132}\text{Sn}$  at point mass radius  $r_{\text{rms}} = 3.80$  fm in a model space of nine major oscillator shells.

Fig. 6 shows that the  $\Delta$ -radial density distribution reaches a peak value of about 0.96 of the proton radial density of  $^{132}\text{Sn}$  evaluated at higher compression an about 0.08 reduced volume ( $r_{\text{rms}} = 2.46$  fm).

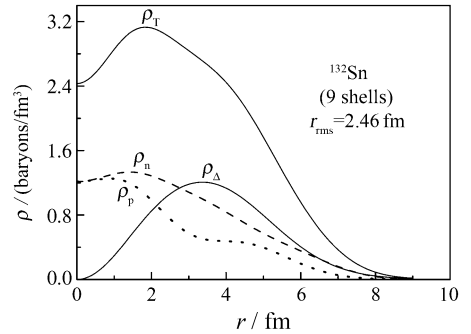


Fig. 6 Total  $\rho_T$ , proton  $\rho_p$  (dotted line), neutron  $\rho_n$  (dashed line), and delta  $\rho_\Delta$  (dotted line) radial density distribution for  $^{132}\text{Sn}$  at point mass radius  $r_{\text{rms}} = 2.46$  fm in a model space of nine major oscillator shells.

If one compares the results here of the radial density distribution with the previous studies<sup>[33, 38, 39, 44]</sup>. It can be found the peak of delta increases as the compression is increased, and also this peak decreases as model space increases.

It can be seen from Figs. 4, 5, and 6, as com-

pression increases the total radial density increases and the radial density distribution of  $\Delta$ 's increases sharply, but radial density of nucleons decreases sharply. If these results are substantial in further work, they could have interesting consequences for subthreshold pion production experiments in nucleus-nucleus collisions where the bombarding energy per nucleon is below that needed to produce pions in free N-N collisions. To the extent these collisions produce isothermal compression and relaxation occurs by decay of the  $\Delta$  to nucleon and pion, these calculations support a collective mechanism for subthreshold pion production. To our knowledge this mechanism has not been previously explored.

It can be seen from Fig. 7 the total radial density for  $^{132}\text{Sn}$  in nine oscillator shells at large compression ( $r_{\text{rms}} = 3.80$  fm) and at equilibrium (point mass radius  $r_{\text{rms}} = 5.63$  fm). This figure shows when the volume of the nucleus is decreased by 0.31 of the equilibrium volume; the radial density increases by about 0.1 of its value at equilibrium case.

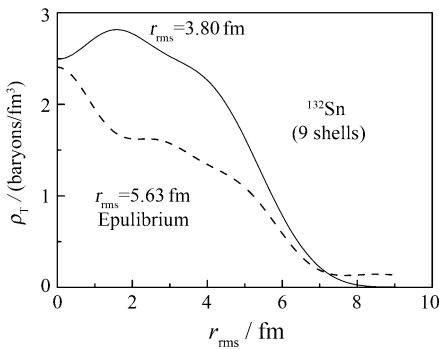


Fig. 7 Total radial density distribution for  $^{132}\text{Sn}$  at equilibrium ( $r_{\text{rms}} = 5.63$  fm) (dashed line) and at  $r_{\text{rms}} = 3.80$  fm (solid line).

The results for the matter distribution of  $^{132}\text{Sn}$  ground state are shown in Fig. 7. For the nucleon distribution, they are difference with the calculation of Fig. 11 in Ref. [33] that is due to different model space.

Clearly, the density in the interior rises relative to the interior density at equilibrium as one

compresses the nucleus. This is in contrast to the behavior of the radial density on the outer-surface, where the radial density distribution is higher at equilibrium than the radial density when the static load is applied.

In Fig. 8, the lowest self-consistent zero-change single particle energy levels as a function of  $r_{\text{rms}}$  were displayed. The orbits is curved up as the load on the nucleus increase. This is because the kinetic energy of the baryons which is positive quantity becomes more influential than the attractive mean field of the baryons. The present results is like results of Fig. 1 of Ref. [38] with same model space and large compression here.

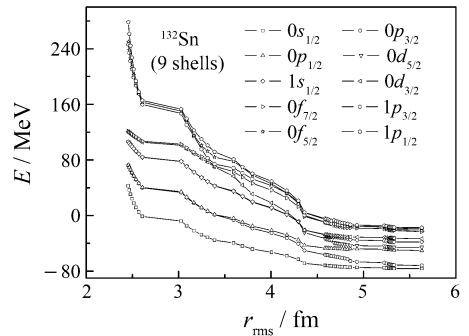


Fig. 8 Single particle energy of the lowest ten neutron states for  $^{132}\text{Sn}$  in nine-oscillator shells as a function of  $r_{\text{rms}}$ .

The single particle energy spectrum also exhibits the gaps between the shells. As the nucleus is compressed, the single particle level ordering and the gaps are preserved. The general trend exhibits the single particle energies (except the deepest bound orbital which actually drops with compression) shift to higher energies as the nucleus is compressed. The curvature goes up more and more as the orbital becomes closer to the surface. This implies that the surface is more responsive to compression than the interior of nucleus.

Recall that single particle spectrum is generated entirely from the underlying microscopic Hamiltonian. Thus, it is a remarkable result of these calculations that the calculated spectrum follows the expected ordering of the phenomenological shell model in the dominantly nucleons orbitals,

and the spectrum exhibits clearly visible gaps between the shells. As the nucleus is compressed, the single particle level ordering and the gaps are preserved. It is also worth noting that the orbitals closest to zero single-particle energy are more sensitive to compression that means there is more responsive of compression than the interior of nucleus. The general trend of single-particle energies exhibits to shift to higher energies as the nucleus is compressed.

The behavior of single particle energy levels is in good agreement with the orbital ordering of the standard shell model. The gap is very clear between the shells. The splitting of the levels in each shell is an indicator that L-S coupling is strong enough in RSC potential, i. e., L-S coupling become stronger as the static load on the nucleus increases. As the nucleus is compressed, the splitting of the orbitals becomes more clear especially in delta orbitals.

## 5 Conclusions

The ground state properties of  $^{132}\text{Sn}$  has been investigated with the  $\Delta$ -degrees of freedom included, using a realistic effective baryon-baryon Hamiltonian within the radial constrained Hartree-Fock approximation with large model space. More nuclear binding energy is found with  $\Delta$ 's included, and about  $4 \times 10^{-4}$  of one  $\Delta$  is found in the ground state (equilibrium) of  $^{132}\text{Sn}$ . The single particle energy levels of the system are evaluated and their behavior under compression is studied. The results for single particle energies at the equilibrium are in agreement with those of the traditional phenomenological shell model.

It can be conclude that the Hartree-Fock energy calculated with a much larger compression decreases as the size of the model space increases for either the N-only or the case including both N and  $\Delta$ . The  $\Delta$  excitation of the nucleon is gradually populated as the nucleus is compressed. The nucleus becomes more compressibility when delta parti-

cle resonances occur. A more modern potential and the inclusion of  $\Delta$  resonances together induce a significant softening of the nuclear equation of state for large amplitude compression.

There is considerable reduction of the zero temperature compressibility when the  $\Delta$  degree of freedom is activated.

Finally, a large fraction of the excitation energy requires to compress the nucleus used to create mass in the form of  $\Delta$ 's. This may have implications for subthreshold pion production in nucleus-nucleus collisions.

## References:

- [1] Chossy T V, Stocker W. Phys Lett, 2001, **B507**: 109.
- [2] Negele J W, Phys Rev, 1970, **C1**: 1260.
- [3] Pasyuk E, Morris C, Ullmann J, *et al.* Acta Phys Pol, 1998, **B29**: 2335.
- [4] Morris C, Zumbro J, McGill J, *et al.* Phys Lett, 1998, **B419**: 25.
- [5] Mosel U, Metag V. Nucl Phys News, 1993, **3**: 25.
- [6] Xiong L, Wu Z, Ko C, *et al.* Nucl Phys, 1990, **A512**: 772.
- [7] Hoffmann M, Mattiello R, Sorge H, *et al.* Phys Rev, 1995, **C51**: 2095.
- [8] Hasan M A, Lee T S H, Vary J P. Phys Rev, 1999, **C61**: 014301.
- [9] Deutchman P A. Aust J Phys, 1999, **52**: 955.
- [10] Terbert C M, Watts D P, Aguar P, *et al.* Phys Rev Lett, 2008, **100**: 132301.
- [11] Fernández de Córdoba P, Oset E, Vicente-Vacas M J. Nucl Phys, 1995, **A592**: 472.
- [12] Badalá A, Barbera R, Bonasera A, *et al.* Phys Rev, 1996, **C54**: R2138.
- [13] Mosel U, Metag V. Nucl Phys News, 1993, **3**: 25.
- [14] Xiong L, Wu Z G, Ko C M, *et al.* Nucl Phys, 1990, **A512**: 772.
- [15] Hoffmann M, Mattiello R, Sorge H, *et al.* Phys Rev, 1995, **C51**: 2095.
- [16] Xing Yongzhong, Zheng Yuming, Srisawad Pornrad, *et al.* Chin Phys Lett, 2009, **26**: 022501.
- [17] Shlomo S, Kolomietz V. Rep Prog Phys, 2005, **68**: 1.
- [18] Frick T, Muther H. Phys Rev, 2005, **C71**: 014313.
- [19] Green A M. Rep Prog Phys, 1976, **39**: 1109.
- [20] Sauer P U. Prog Nucl Part Phys, 1986, **16**: 35.
- [21] Valcare A, Fernández F, Garcilazo H, *et al.* Phy Rev, 1996,

- C49**; 1799.
- [22] Klimkiewicz A, Paar N, Adrich P, *et al.* Acta Phys Pol, 2009, B **40**: 589.
- [23] Coraggio L, Covello A, Gargano A, *et al.* Nucl Phys, 2008, **A805**: 424c.
- [24] Sarkar S, Sarkar M. Phys Rev, 2008, **C78**: 024308.
- [25] Brandow H B. Rev Mod Phys, 1967, **39**: 77.
- [26] Lee T. Phys Rev Lett, 1983, **20**: 1571.
- [27] Lee T. Phys Rev, 1994, **C29**: 195.
- [28] Lee T, Matsuyama A. Phys Rev, 1985, **C32**: 516.
- [29] Lee T, Matsuyama A. Phys Rev, 1987, **C36**: 1459.
- [30] Matsuyama A, Lee T. Phys Rev, 1986, **C34**: 1900.
- [31] Matsuyama A, Lee T. Nucl Phys, 1991, **A526**: 547.
- [32] Hasan M A, Lee T S H, Vary J P. Phys Rev, 1997, **C56**: 3063.
- [33] Hasan M A, Vary J P, Lee T S H. Phys Rev, 2001, **C64**: 024306.
- [34] Barrett B, Stetcu I, Navrátil P, *et al.* J Phys A: Math. Gen, 2006, **39**: 9983.
- [35] Hasan M A, Köhler S H, Vary J P. Phys Rev, 1987, **C36**: 2180.
- [36] Hasan M A, Köhler S H, Vary J P. Phys Rev, 1987, **C36**: 2649.
- [37] Vary J P, Hasan M A. Phys Rep, 1994, **242**: 139.
- [38] Vary J P, Hasan M A. Nucl Phys, 1994, **A570**: 355.
- [39] Hasan M A, Dirasat. University of Jordan, 1995, **22**: 777.
- [40] Hasan M A, Vary J P. Phys Rev, 1994, **C50**: 202.
- [41] Hasan M A, Vary J P. Phys Rev, 1996, **C54**: 3035.
- [42] Abu-Sei'leek M H, Hasan M A, Comm Theort Phys, 2010, **54**: 339.
- [43] Abu-Sei'leek M H. Comm Theort Phys, 2010, in press.
- [44] Abu-Sei'leek M H. Pramana-Journal of Physics, 2010, in press.
- [45] Tzeng Y, Kuo T, Lee T. Physica Scripta, 1996, **53**: 300.
- [46] Reid R V, Ann Phys (N. Y. ), 1968, **50**: 411.
- [47] Gari M, Niephaus G, Sommer B. Phys Rev, 1981, **C23**: 504.
- [48] Navrátil P, Ormand W. Phys Rev, 2003, **C68**: 034305.
- [49] Stetcu I, Barrett B, Navrátil P, *et al.* Int J Mod Phys, 2004, E **14**: 95.
- [50] Vary J, Atramentov O V, Barrett B R, *et al.* Eur Phys J, 2005, **A25**: 475.
- [51] Hasan M, Vary J, Navrátil P. Phys Rev, 2004, **C69**: 034332.
- [52] Bozzolo G, Vary J. Phys Rev Lett, 1984, **53**: 903.
- [53] Bozzolo G, Vary J. Phys Rev, 1985, **C31**: 1909.
- [54] Saraceno M, Bozzolo J P, Miller H G. Phys Rev, 1988, **C37**: 1267.
- [55] Mosol U, Metag V. Nucl Phys News, 1993, **3**: 25.
- [56] Xiong L, Ko C M, Nucl Phys, 1990, **A512**: 772.
- [57] Hoffmann M. *et al.* Phys Rev, 1995, **C51**: 2095.